

25th ABCM International Congress of Mechanical Engineering
October 20-25, 2019, Uberlândia, MG, Brazil

COB-2019-0106

OPTIMAL INTERPLANETARY TRAJECTORIES USING THE TWO-BODY, FOUR-BODY, AND, FIVE-BODY PROBLEMS

Luiz Arthur Gagg Filho
Sandro da Silva Fernandes

Instituto Tecnológico de Aeronáutica, Praça Marechal Eduardo Gomes 50, Vila das Acácias, 12228-900, São José dos Campos-SP, Brazil
arthurga@ita.br, sandro@ita.br

Abstract. *This work formulates an interplanetary transfer problem from a circular low Earth orbit (LEO) to a circular low orbit around a target planet (Mars or Venus) by using two impulses tangential to the terminal orbits. Models based on the two-body, four-body, and, five-body problems are considered. Among the models based on the two-body problem there are the interplanetary patched-conic approximation based on the Hohmann transfer; the interplanetary patched-conic approximation based on the Gauss problem; and, the patched-conic approximation based on a detailed geometry which can include a swing-by maneuver with the Moon. In the context of the restricted four-body problem (Sun-Earth-target planet-space vehicle), the present work formulates the transfer problem utilizing Cartesian coordinates in three sets of differential equations of motion to improve the integrator sensitivity. A two-point boundary value problem and two optimization problems, with one or two degrees of freedom, are enunciated. Thus, optimal trajectories are determined in order to minimize the fuel consumption. The lunar swing-by maneuver is then formulated in a five-body problem. The optimal trajectories are compared among the models with and without lunar swing-by maneuver. The results show that the saving of fuel consumption due to the lunar swing-by maneuver is substantial with no greater changes in the time of flight.*

Keywords: *interplanetary transfer, optimal trajectory, lunar swing-by, four-body problem, five-body problem*

1. INTRODUCTION

Private companies together with governmental agencies are scheduling spectacular manned missions to Moon. The success of these missions represents a huge step to achieve a greater accomplishment: a manned mission to Mars and its future colonization. Companies like Boeing, Lockheed Martin and Space X want to be the pioneers on these explorations. As an example, NASA and Lockheed Martin company, which are responsible for the construction of a space vehicle named Orion, have revealed a tight schedule of activities (Cichan *et al.*, 2016).

While manned missions are still not performed in interplanetary space, unmanned missions are exploring the Solar System for several reasons: economic (asteroid mining), colonization perspective (Mars colonization), survival purpose (the studying of dangerous asteroids that could impact Earth), and, scientific purposes (life searching). At the moment, Enceladus (moon of Saturn) and Europa (moon of Jupiter) are the main candidates to support life. In this way, missions are being planned for both moons (Konstantinidis *et al.*, 2015; Jones, 2016). Despite the several future planes, the unmanned missions are limited to the Solar System, and, the manned missions are still limited to the low orbits around the Earth. A few cogitate about interstellar missions: the Breakthrough Starshot project (Daukantas, 2017) intends to send a probe to reach Proxima Centauri, but several technological advances are needed.

In the context of space missions, the present work proposes models based on the two-body, four-body, and, five-body problems for trajectory determinations in a preliminary mission analysis from Earth to inner planets (Venus) and outer planets (Mars) considering the planar models. Among the models based on the two-body problem there are the interplanetary patched-conic approximation based on the Hohmann transfer, which solves the heliocentric phase; and, the interplanetary patched-conic approximation based on the Gauss problem (Bate *et al.*, 1971). The characterization of the trajectory phases by the patched-conic approximations is accomplished by the definition of the Sphere of Influence (SOI), in a way that, when the motion of the space vehicle occurs, for instance, inside the Earth's SOI the geocentric phase is characterized.

Nevertheless, despite the patched-conic approximations based on the Hohman transfer and the one based

on the Gauss problem being usually used for preliminary mission analysis, these models patch the trajectory phases in an independent way. In this way, the visualization of the complete trajectory has discontinuities and informations related to the complete trajectory are lost. In this sense, the present work also utilizes a patched-conic approximation based on a detailed geometry of the transfer problem (Gagg Filho and da Silva Fernandes, 2018) which determines the complete trajectory by means of a two-point boundary value problem (TPBVP), and, it includes a swing-by maneuver with the Moon. Broucke (1988) qualitatively mentions that the Moon is a weak gravitational accelerator; however, the present work extends the conclusion of Broucke (1988) by quantifying the saving of the fuel consumption, represented by the sum of the velocity increments, when a lunar swing-by maneuver is performed in an interplanetary mission.

In the context of the interplanetary transfer model based on the planar restricted four-body problem (PCR4BP, Sun-Earth-target planet-space vehicle), the present work formulates the same transfer problem with a different approach from the one described by Miele and Wang (1999), i.e, the differential equations that governs the motion of the space vehicle are written, in the present work, utilizing Cartesian coordinates (Miele and Wang (1999) utilize polar coordinates) in three distinct forms in order to improve the integrator sensitivity. Each form defines the differential equations for the relative motion of the space vehicle with respect to Earth, Sun, and target planet, respectively. The choice of the properly version of the differential equations is dependent on the predominant gravitational field on the space vehicle. A two-point boundary value problem (TPBVP), involving prescribed values of the initial phase angle between the space vehicle and the Earth and the initial phase angle (rendez-vous angle) of the target planet, is formulated. Based on this TPBVP, an one-degree of freedom optimization problem is enunciated to minimize the total fuel consumption with a prescribed rendez-vous angle. A two-degree of freedom optimization problem is then formulated, in which the rendez-vous angle is also an unknown to be determined in order to minimize the fuel consumption. Next, the Moon's gravitational influence is included in the set of differential equations that describes the relative motion of the space vehicle to Earth; thus, the four-body problem is converted in a five-body problem in the neighborhood of the Earth. Therefore, this last model enables the lunar swing-by maneuver before the leaving of the space vehicle from the Earth's SOI.

2. OBJECTIVES

This work analyses the Earth-Mars and Earth-Venus transfers from a circular low Earth orbit (LEO) to a circular low orbit around the target planet (Venus or Mars) by using bi-impulsive optimal trajectories that minimize the fuel consumption in the context of the two-body, four-body, and, five-body problems. This work also investigates the saving of fuel consumption if a lunar swing-by maneuver is performed in these missions.

3. FORMULATION

This section formulates the interplanetary transfer based on the two-body problem, the restricted four-body problem, and, the restricted five-body problems. The interplanetary mission consists in transferring a space vehicle from a low Earth orbit (*LEO*) to a low Mars orbit - *LM_tO* (or to a low Venus orbit - *LVO*) by applying two impulses tangential to the terminal orbits. The first velocity increment Δv_{LEO} inserts the space vehicle into a transfer trajectory, and, the second velocity increment Δv_{LM_tO} (or Δv_{LVO}) brakes the vehicle circularizing its motion at the *LM_tO* (or *LVO*). The fuel consumption is represented by the total characteristic velocity $\Delta v_{Total} = \Delta v_{LEO} + \Delta v_{LM_tO}$ (or $\Delta v_{LEO} + \Delta v_{LVO}$) (Marec, 1979). The terminal orbits, the planet orbits and the Moon orbit are considered circular and coplanar, in a way that, the motion of the space vehicle occurs in the plane of the orbits.

Among the models based on the two-body problem there are: the patched-conic based on the Hohmann transfer, the patched-conic based on the Gauss problem, the patched-conic with detailed geometry, and, the patched-conic with a lunar swing-by maneuver. For all the models based on patched-conic approximations, the interplanetary trajectory is divided in phases, which are defined by the sphere of influence (SOI) of the main bodies. In this way, the patched-conic approximations have, at least, three phases: the geocentric phase, where only the gravitational field of the Earth is considered; the heliocentric phase, where only the gravitational field of the Sun is considered; and, the planetocentric phase, where only the gravitation field of the target planet is considered. These models are shortly discussed below. In order to simplify the notations of formulation, Mars is considered to be the target planet without loss of generalization.

3.1 Patched-conic based on the Hohmann transfer

For the patched-conic based on the Hohmann transfer, the heliocentric phase is solved first. For this phase, the Hohmann transfer (Prussing and Conway, 1993; Bate *et al.*, 1971) is utilized to estimate the parameters of the

elliptic transfer trajectory that defines the heliocentric phase, which include the Hohmann velocity increments $\Delta v_{0,Hohmann}$ and $\Delta v_{f,Hohmann}$. Next the geocentric and the planetocentric are, simultaneously, determined by considering them as hyperbolic trajectories with their excess velocity, $\Delta v_{\infty,geo}$ and $\Delta v_{\infty,pla}$ respectively, equal to the Hohmann velocity increments, $\Delta v_{0,Hohmann}$ and $\Delta v_{f,Hohmann}$. By using well-known results of the two-body problem, it is now possible to determine the initial velocity, v_0 , of the space vehicle right after the application of Δv_{LEO} , and the final velocity, v_f , of the space vehicle right before the application of Δv_{LM_tO} (or Δv_{LVO}). Then, the velocity increments are calculated as below:

$$\Delta v_{LEO} = v_0 - \sqrt{\frac{\mu_E}{r_0}} \quad (1)$$

$$\Delta v_{LM_tO} = v_f - \sqrt{\frac{\mu_{M_t}}{r_f}} \quad (2)$$

where μ_E and μ_{M_t} are the Earth and Mars gravitational parameters, respectively; r_0 is radius of the *LEO*, i.e., $r_0 = R_E + h_{LEO}$ with R_E and h_{LEO} being the Earth's radius and the altitude of the *LEO*, respectively; r_f is radius of the *LM_tO*, i.e., $r_f = R_{M_t} + h_{LM_tO}$ with R_{M_t} and h_{LM_tO} being the Mars's radius and the altitude of the *LM_tO*, respectively.

3.2 Patched-conic based on the Gauss problem

In the previous section, the space vehicle describes an elliptic heliocentric trajectory making a 180° arc of true anomaly according to the Hohmann transfer. However, if it is desired to reach the SOI of Mars with a smaller time travel, a smaller arc of true anomaly must be obtained. In this way, the vectors of the excess velocities must be obtained by another procedure. To achieve this goal, the heliocentric phase is solved with the Gauss problem (Bate *et al.*, 1971). Using the Gauss problem, the magnitude of two position vectors of the space vehicle must be provided as well as the time of flight and the true anomaly variation Δf between these two vector, and, the direction of motion. Since the elliptic trajectory is defined from the boundary of the Earth's SOI to the boundary of Mars' SOI, the magnitudes of these two vectors are the Earth-Sun distance, D_E , and the Mars-Sun distance, D_{M_t} . Once the excess velocity, $\Delta v_{0,Gauss}$ and $\Delta v_{f,Gauss}$, are obtained based on the Gauss problem, the initial velocity v_0 and the final velocity v_f of the space vehicle are calculated; and, the velocity increments, Δv_{LEO} and Δv_{LM_tO} , applied to the space vehicle, are determined using Eqs. (1) and (2), respectively.

Note that the Gauss problem is solved for a prescribed value of time of flight; therefore, an optimization problem is enunciated below by setting the time of flight as an unknown to be determined in order to obtain the solution with minimum Gauss velocity increment $\Delta v_{Total,Gauss}$.

Problem 1 “Given the value of Δf , the direction of motion, and, prescribing the magnitudes of two position vectors (D_E and D_{M_t} , for instance), determine the time of flight Δt between these two vectors that minimizes the function

$$F(\Delta t) : \quad \Delta v_{Total,Gauss} = \Delta v_{0,Gauss} + \Delta v_{f,Gauss} \quad (3)$$

3.3 Patched-conic with detailed geometry

In the patched-conic approximations based on the Hohmann transfer and the one based on the Gauss problem, the heliocentric phase is first solved such that the excess velocities are determined. For these models, it is not possible to build the complete Earth-Mars trajectory without discontinuity between the points that connects the phases. In this way, this section shortly comments about a new patched-conic approximation in which the excess velocities are determined through a detailed geometry and it is based on an extension of the lunar patched-conic approximation, as described by Gagg Filho and da Silva Fernandes (2015). For this model, the geocentric phase is solved first, followed by the heliocentric phase, and, finally, the planetocentric is determined. Therefore, when the complete trajectory, Fig. 1, is determined, one must compare the calculated arrival condition of the space vehicle with the prescribed arrival condition. In this way, the complete trajectory is obtained by solving a two-point boundary value problem (TPBVP) as enunciated below

Problem 2 “Given the terminal altitudes h_{LEO} and h_{LM_tO} , and, prescribing the initial phase angle $\theta_{EP}(0)$ of the space vehicle with the Earth and the phase angle λ_{M_t} , which describes the arrival geometry at the Mars' SOI, determine the initial velocity v_0 subjected to the final constraint:

$$g(v_0) : \quad r_{p_{pla}} - r_f = 0 \quad (4)$$

where $r_{p_{pla}}$ is the calculated pericenter distance of the planetocentric phase; and, r_f is the prescribed radius of the LM_tO .”

The velocity increments, Δv_{LEO} and Δv_{LM_tO} , applied to space vehicle are determined using Eqs. (1) and (2), respectively. Note that an optimization problem can be enunciated in order to determine the value of λ_{Mt} that minimizes the fuel consumption Δv_{Total} .

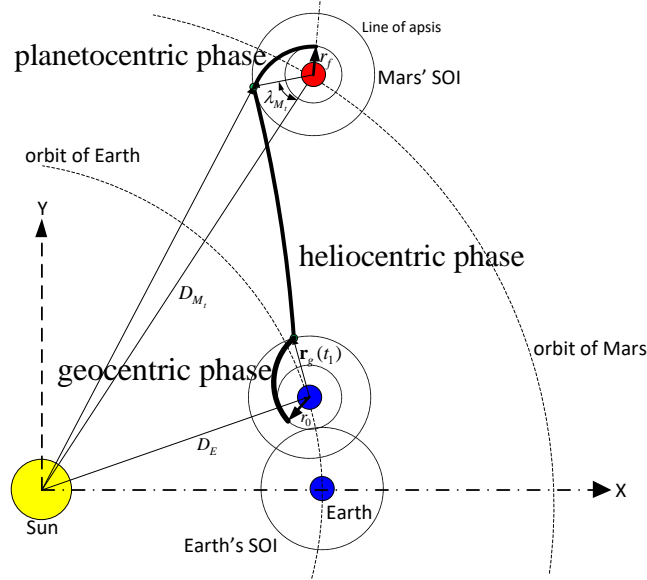


Figure 1: Geometry of the patched-conic approximation.

3.4 Patched-conic with a lunar swing-by maneuver

This patched-conic model is similar to the patched-conic approximation presented in section 3.3, but with two more phases in order to include a lunar swing-by maneuver (see Fig. 2). In this way, the complete trajectory is described by five phases: a first elliptic geocentric phase is characterized from the departure of the space vehicle from the LEO until it reaches the boundary of the Moon’s SOI; next, an hyperbolic selenocentric phase models the lunar swing-by maneuver; a second, but hyperbolic, geocentric phase is defined from the departure from the Moon’s SOI until the reaching of the boundary of the Earth’s SOI; next, an elliptic heliocentric phase is defined from the departure of the Earth’s SOI until the space vehicle reaches the Mars’ SOI; finally, the hyperbolic planetocentric phase is characterized from the boundary of the Mars’ SOI until the arrival at the LM_tO . The complete formulation of this patched-conic approximation can be found in Gagg Filho and da Silva Fernandes (2018). Since there is a lunar swing-by maneuver in this model, an intermediary constraint is included. This constraint defines the pericenter altitude of the selenocentric phase. Therefore, the TPBVP can be enunciated as it follows:

Problem 3 “Given the terminal altitudes h_{LEO} and h_{LM_tO} , and, prescribing the phase angle λ_1 , which describes the arrival geometry at the Moon’s SOI, and the phase angle λ_{Mt} , which describes the arrival geometry at the Mars’ SOI, determine the initial velocity v_0 and the phase angles λ_S , which describes the departure geometry from the Earth’s SOI, subjected to the final constraint:

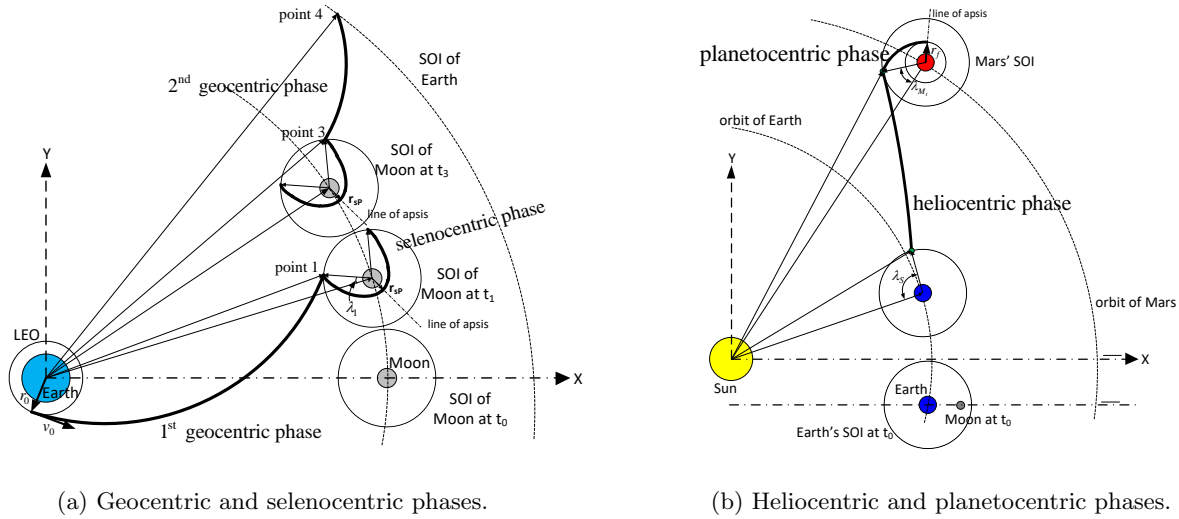
$$g(\lambda_S) : r_{p_{pla}} - r_f = 0 \quad (5)$$

and, to the intermediary constraint:

$$g_0(v_0) : r_{pM} - r_{sP} = 0 \quad (6)$$

where r_{sP} is the prescribed distance of close encounter with the Moon, and, r_{pM} is the calculated pericenter distance of the selenocentric phase.”

The velocity increments, Δv_{LEO} and Δv_{LM_tO} , applied to space vehicle are determined using Eqs. (1) and (2), respectively. Note that, an optimization problem with two-degree of freedom can be enunciated in order to determine the values of λ_{Mt} and λ_1 which minimize the fuel consumption Δv_{Total} .



(a) Geocentric and selenocentric phases. (b) Heliocentric and planetocentric phases.
Figure 2: Patched-conic approximation with swing-by. Modified from Gagg Filho and da Silva Fernandes (2018).

3.5 Interplanetary transfer problem based on the four-body problem

This section formulates the interplanetary transfer problem based on the planar circular restricted four-body problem (PCR4BP), in which the three primaries are the Earth, the Sun and Mars, and, the fourth body is the space vehicle. A mathematical development can be found in Miele and Wang (1999), which utilizes polar coordinates to formulate the problem; however, the present work formulates the differential equations utilizing cartesian coordinates. To solve the interplanetary transfer problem, consider an inertial reference frame S_{XY} centered at the Sun with the X -axis pointing to Earth at the initial time t_0 , and with the Y -axis ortogonal to the X -axis at the direction of orbital motion of the Earth around the Sun. Despite the space vehicle being subjected to the gravitational fields of the three primaries during the whole trajectory, three phases of the trajectories are considered to formulate the problem: the geocentric phase, the heliocentric phase, and, the planetocentric phase. The division in three phases is performed in order to facilitated the integration of the differential equations, which are accomplished with variable normalization suitable for each phase. For example, when the space vehicle is at the neighborhood of Earth, the gravitational field of this body is predominant, thus, the system of differential equations is written based on the relative motion of the space vehicle with respect to Earth. In this case, the normalization is performed by utilizing the Earth's parameters. On the other hand, when the space vehicle is far from Earth and Mars, the gravitational field of the Sun is predominant; therefore, the system of differential equations is written based on the relative motion of the space vehicle with respect to Sun. It follows the same explanation when the space vehicle is at the neighborhood of Mars. In order to characterize the phases and to switch the versions of differential equations the concept of SOI is utilized. Note that the concept of SOI in this model is utilized solely to separe the phases; thus, even when the space vehicle is inside a specific SOI, the vehicle is still subject to the three gravitational fields of the primaries.

3.5.1 Geocentric phase

At the initial time, the space vehicle is at the LEO . After applying the first velocity increment Δv_{LEO} , the space vehicle is inserted into an interplanetary transfer trajectory. So, at the beginning of the mission, the space vehicle is at the neighborhood of the Earth and its motion is described by the following system of differential equations:

$$\ddot{x}_{EP} = -\frac{\mu_S}{r_P^3}(x_{EP} + x_E) - \frac{\mu_E}{r_{EP}^3}(x_{EP}) - \frac{\mu_{M_t}}{r_{M_tP}^3}(x_{EP} + x_E - x_{M_t}) + \frac{\mu_S}{r_E^3}(x_E) \quad (7)$$

$$\ddot{y}_{EP} = -\frac{\mu_S}{r_P^3}(y_{EP} + y_E) - \frac{\mu_E}{r_{EP}^3}(y_{EP}) - \frac{\mu_{M_t}}{r_{M_tP}^3}(y_{EP} + y_E - y_{M_t}) + \frac{\mu_S}{r_E^3}(y_E) \quad (8)$$

where (x_{EP}, y_{EP}) are the components of the position vector of the space vehicle with respect to Earth; (x_E, y_E) and (x_{M_t}, y_{M_t}) define the components of the position vector of the Earth and Mars, respectively; r_P , r_{EP} , and, r_{M_tP} are the magnitude of the position vector of the space vehicle with respect to, respectively, Sun, Earth, and the target planet (Mars), and, μ_S is the gravitational parameter of the Sun.

The initial conditions of the system defined by Eqs. (7) and (8) correspond to the components of the position and velocity vectors of the space vehicle with respect to Earth at t_0 , which is time right after the application of Δv_{LEO} .

3.5.2 Heliocentric phase

In this phase, the gravitational field of the Sun is predominant and it begins when the space vehicle leaves the Earth's SOI. In this way, the system of differential equations that describes the motion of the space vehicle is written with its position and velocity vectors with respect to the inertial frame as following:

$$\ddot{x}_P = -\frac{\mu_S}{r_P^3} x_P - \frac{\mu_E}{r_{EP}^3} (x_P - x_E) - \frac{\mu_{M_t}}{r_{M_tP}^3} (x_P - x_{M_t}) \quad (9)$$

$$\ddot{y}_P = -\frac{\mu_S}{r_P^3} y_P - \frac{\mu_E}{r_{EP}^3} (y_P - y_E) - \frac{\mu_{M_t}}{r_{M_tP}^3} (y_P - y_{M_t}) \quad (10)$$

where (x_P, y_P) are the components of the position vector of the space vehicle with respect to Sun (origin of the inertial reference system).

The initial conditions of the system defined by Eqs. (9) and (10) are the components of the position and velocity vectors of the space vehicle with respect to Sun at time t_1 , which is the time instant when the integration of the geocentric phase is completed.

3.5.3 Planetocentric phase

The planetocentric phase begins when the space vehicle reaches the boundary of Mars' SOI; thus, the gravitational field of Mars is predominant. The system of differential equations is expressed with the components of the position and velocity vectors of the space vehicle with respect to Mars as below:

$$\ddot{x}_{M_tP} = -\frac{\mu_S}{r_P^3} (x_{M_tP} + x_{M_t}) - \frac{\mu_E}{r_{EP}^3} (x_{M_tP} + x_{M_t} - x_E) - \frac{\mu_{M_t}}{r_{M_tP}^3} (x_{M_tP}) + \frac{\mu_S}{r_{M_t}^3} (x_{M_t}) \quad (11)$$

$$\ddot{y}_{M_tP} = -\frac{\mu_S}{r_P^3} (y_{M_tP} + y_{M_t}) - \frac{\mu_E}{r_{EP}^3} (y_{M_tP} + y_{M_t} - y_E) - \frac{\mu_{M_t}}{r_{M_tP}^3} (y_{M_tP}) + \frac{\mu_S}{r_{M_t}^3} (y_{M_t}) \quad (12)$$

where (x_{M_tP}, y_{M_tP}) are the components of the position vector of the space vehicle with respect to Mars. The initial conditions of the system defined by Eqs. (11) and (12) are the components of the position and velocity vectors of the space vehicle to Mars at time t_2 , which is the time instant at the end of the heliocentric phase. Note that, in order to switch between the phases, the position vector of the primaries must be monitored. The planetocentric phase occurs between $t = t_2$ and $t = T$, where T is the total time of flight of the complete trajectory.

3.5.4 Two-point boundary value problem

According to the sections 3.5.1 - 3.5.3, one can determine the trajectory by integrating the system of differential equations of each phase if the initial conditions of Eqs. (7) and (8) are given. However the final conditions must agree to the arrival conditions at the LM_tO . Therefore, a TPBVP is enunciated as it follows:

Problem 4 "Given the terminal altitudes h_{LEO} and h_{LM_tO} , and, prescribing the initial phase angle $\theta_{EP}(0)$ of the space vehicle with respect to Earth and the initial phase angle of Mars $\theta_{M_t}(0)$, determine the set of variables $(\Delta v_{LEO}, \Delta v_{LM_tO}, T)$ subjected to the final constraints:

$$g_1 : (x_{M_tP}(T))^2 + (y_{M_tP}(T))^2 - (r_{M_tP}(T))^2 = 0 \quad (13)$$

$$g_2 : (\dot{x}_{M_tP}(T))^2 + (\dot{y}_{M_tP}(T))^2 - \left[\sqrt{\frac{\mu_{M_t}}{r_{M_tP}(T)}} + \Delta v_{LM_tO} \right]^2 = 0 \quad (14)$$

$$g_3 : (x_{M_tP}(T))(\dot{y}_{M_tP}(T)) - (y_{M_tP}(T))(\dot{x}_{M_tP}(T)) \pm r_{M_tP}(T) \left[\sqrt{\frac{\mu_{M_t}}{r_{M_tP}(T)}} + \Delta v_{LM_tO} \right] = 0 \quad (15)$$

where the higher (lower) signal in Eq. (15) indicates a clockwise (counterclockwise) arrival at the LM_tO .

3.5.5 Two-degree optimization problem

According to problem 4, the phase angles $\theta_{EP}(0)$ and $\theta_{M_t}(0)$ must be prescribed in order to solve the TPBVP. However one can set these phase angles as unknowns to solve a two-degree optimization problem as enunciated below:

Problem 5 “Given the terminal altitudes h_{LEO} and h_{LM_tO} , determine the set of variables $(\Delta v_{LEO}, \Delta v_{LM_tO}, T, \theta_{EP}(0), \theta_{M_t}(0))$ that minimizes the function

$$F : \quad \Delta v_{Total} = \Delta v_{LEO} + \Delta v_{LM_tO} \quad (16)$$

subjected to the final constraints g_1, g_2 and g_3 defined by Eqs. (13), (14) and (15), respectively.”

3.6 Interplanetary transfer problem based on the five-body problem

This model extends the formulation of the interplanetary transfer based on the PCR4BP (section 3.5) by including a lunar swing-by maneuver. In this sense the system of differential equations of the geocentric phase, Eqs. (7) and (8), is modified by adding the gravitational attraction of the Moon converting the PCR4BP into a planar circular restricted five-body problem (PCR5BP). Thus, the new system of differential equations that describes the motion of the space vehicle at the neighborhood of Earth is described as below:

$$\ddot{x}_{EP} = -\frac{\mu_S}{r_P^3}(x_{EP} + x_E) - \frac{\mu_E}{r_{EP}^3}(x_{EP}) - \frac{\mu_{M_t}}{r_{M_tP}^3}(x_{EP} + x_E - x_{M_t}) - \frac{\mu_M}{r_{PM}^3}(x_{EP} - x_{ME}) + \frac{\mu_S}{r_E^3}(x_E) \quad (17)$$

$$\ddot{y}_{EP} = -\frac{\mu_S}{r_P^3}(y_{EP} + y_E) - \frac{\mu_E}{r_{EP}^3}(y_{EP}) - \frac{\mu_{M_t}}{r_{M_tP}^3}(y_{EP} + y_E - y_{M_t}) - \frac{\mu_M}{r_{PM}^3}(y_{EP} - y_{ME}) + \frac{\mu_S}{r_E^3}(y_E) \quad (18)$$

where (x_{ME}, y_{ME}) are the components of the position vector of the Moon with respect to Earth, and, r_{PM} is the magnitude of the position vector of the space vehicle with respect to Moon.

When the space vehicle leaves the Earth’s SOI, the system of differential equation must be rewritten with the position vector of the space vehicle with respect to Sun in a similar way to Eq. (17) and (18). In the same way, when the space vehicle enters the SOI of the target planet, another system of differential equations is used with the position vector of the space vehicle with respect to the target planet. To simplify numerical computation the gravitational field of the Moon is neglected in the heliocentric and planetocentric phases.

3.6.1 The Two-Point Boundary Value Problem (TPBVP)

The TPBVP of this interplanetary transfer problem is similar to the one based on the four-body problem, but with an additional parameter: the initial phase angle of the Moon $\theta_M(0)$ with respect to the X -axis of the inertial reference frame. Therefore, the TPBVP is enunciated as:

Problem 6 “Given the terminal altitudes h_{LEO} and h_{LM_tO} , and, prescribing the phase angles $\theta_{EP}(0), \theta_{M_t}(0)$, and $\theta_M(0)$, determine the set of variables $(\Delta v_{LEO}, \Delta v_{LM_tO}, T)$, subjected to the final constraints g_1, g_2 and g_3 defined by Eqs. (13), (14) and (15), respectively.”

Note that an optimization problem of two-degree of freedom is also formulated as problem 5 but with $\theta_M(0)$ as a prescribed parameter. Moreover, one can set $\theta_M(0)$ as an unknown to be determined in a three-degree optimization problem.

4. RESULTS

This section shows briefly results about Earth-Mars and Earth-Venus missions. The TPBVPs are solved by means of a Newton-Raphson algorithm, and, the optimization problems are solved by means of a Sequential Gradient Restoration Algorithm (Miele *et al.*, 1969). The computational codes are implemented using FORTRAN 90. Table 1 compares interplanetary trajectories with minimum fuel consumption for an Earth-Mars mission with and without lunar swing-by maneuvers. Several models are considered: patched-conic approximations, four-body problem, and, five-body problem. The altitudes of the departure and arrival orbits are 463 km and 200 km, respectively. Figure 3 plots the trajectory considering the patched-conic approximation with a lunar swing-by maneuver and the trajectory in the context of five-body problem with a lunar swing-by maneuver as well. The swing-by maneuver is better visualized in a Earth-Moon rotating reference centered at Earth as depicted in Fig. 4.

Table 1: Minimum fuel consumption trajectories for Earth-Mars mission.

Model	Δv_{LEO} [km/s]	Δv_{LM_iO} , [km/s]	Δv_{Total} [km/s]	Time of Flight [days]	$\theta_{M_t}(T)$, [degrees]	$\theta_{EP}(0)$ [degrees]
PCR4BP ^[1]	3.551905	2.100124	5.652029	257.861	179.075	298.382
Miele ^[2]	3.552000	2.100000	5.652000	257.880	179.020	298.150
<i>patched-conic</i> based on Hohmann	3.555746	2.101260	5.657006	264.430	182.888	299.474
<i>patched-conic</i> based on Gauss	3.555572	2.101454	5.657026	263.579	179.505	299.139
<i>patched-conic</i> detailed geometry	3.514668	2.087434	5.602101	257.965	178.070	297.573
<i>patched-conic</i> with lunar swing-by ^[3]	3.36221	2.086891	5.449101	257.443	132.079	218.965
<i>PCR5BP</i> with lunar swing-by	3.415512	2.097689	5.513202	260.455	179.885	265.154

^[1] Results from a two degree-of-freedom optimization problem.

^[2] Results based on the PR4CP calculated by Miele and Wang (1999).

^[3] Results based on the patched-conic approximation by Gagg Filho and da Silva Fernandes (2018).

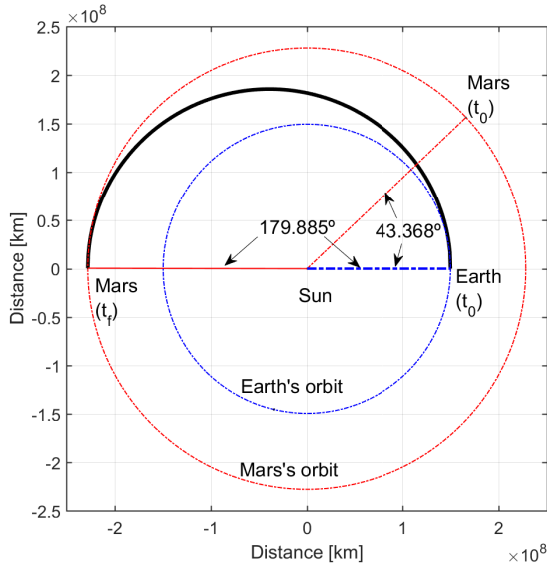


Figure 3: Complete Earth-Mars trajectory in the inertial reference frame.

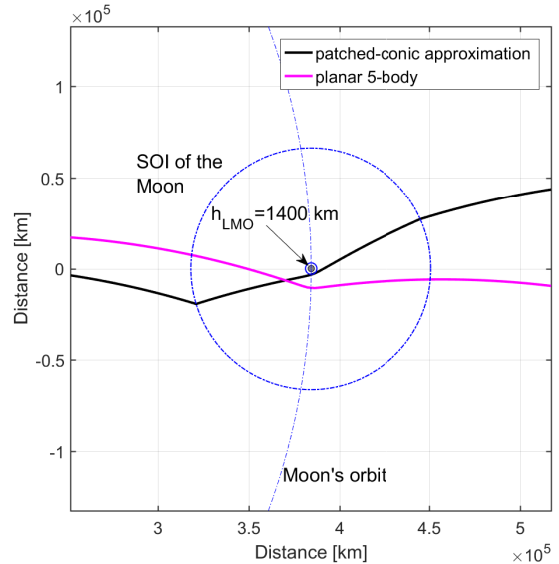


Figure 4: Zoom at the lunar swing-by in the Earth-Moon rotating reference frame. h_{LMO} is the swing-by closest approach altitude.

Tables 1 and 2 show that the saving of fuel consumption due to the lunar swing-by maneuver is substantial and not followed by greater changes in the time of flight. Indeed, for the Earth-Mars mission, the total velocity increment of the trajectory in the PCR5BP (with lunar swing-by) is 138.827 m/s smaller than the trajectory in the PCR4BP (without lunar swing-by) with a time of flight of only 2.594 days longer. For Earth-Venus mission, the total velocity increment of the trajectory in the PCR5BP is 170.034 m/s smaller than the trajectory in the PCR4BP with a time of flight of only 3.069 days longer. Note that the fuel consumption in the PCR5BP is 50.027 m/s smaller than the patched-conic approximation with lunar swing-by for the Earth-Venus mission. On the other hand, for Earth-Mars mission, the fuel consumption in the PCR5BP is 64.101 m/s larger than the patched-conic approximation with lunar swing-by. Despite these differences between the models, it is clear that the lunar swing-by maneuver saves considerable fuel consumption for both Earth-Mars and Earth-Venus missions.

Despite the fuel consumption be different between the PCR5BP and the patched-conic approximation with lunar swing-by, the complete trajectories of both models are practically coincident as it is shown by Fig. 3 for Earth-Mars mission and by Fig. 5 for Earth-Venus mission. The difference between trajectories, when both models are compared, is better visualized in the swing-by maneuver as shown in Figs. 4 and 6, respectively, for Earth-Mars and Earth-Venus missions. Note that, even when the PCR5BP trajectories perform lunar swing-by

maneuvers with, practically, the same altitude as the patched-conic approximation as in Fig. 6, the swing-by maneuver trajectories between the models do not coincide. This small difference between the swing-by maneuvers causes large changes on the phase $\theta_{EP}(0)$ (Tab. 1 and 2), even when the same reference frame is utilized.

Table 2: Minimum fuel consumption trajectories for Earth-Venus mission.

Model	Δv_{LEO} [km/s]	Δv_{LVO} , [km/s]	Δv_{Total} [km/s]	Time of Flight [days]	$\theta_V(T)$, [degrees]	$\theta_{EP}(0)$ [degrees]
PCR4BP ^[1]	3.449138	3.337284	6.786422	139.628	173.795	105.084
<i>patched-conic</i> based on Hohmann	3.447245	3.339810	6.787055	151.822	189.273	115.420
<i>patched-conic</i> based on Gauss	3.447417	3.339550	6.786967	151.771	189.197	115.355
<i>patched-conic</i> detailed geometry	3.585543	3.326100	6.911643	124.337	157.157	79.189
<i>patched-conic</i> with lunar swing-by ^[2]	3.376566	3.289849	6.666415	149.440	269.358	208.679
<i>PCR5BP</i> with lunar swing-by	3.259056	3.357333	6.616388	142.697	172.727	66.024

^[1] Results from a two degree-of-freedom optimization problem.

^[2] Results based on the patched-conic approximation by Gagg Filho and da Silva Fernandes (2018).

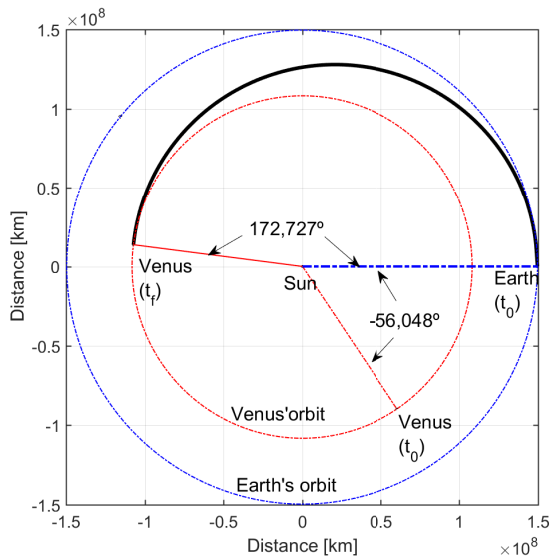


Figure 5: Complete Earth-Venus trajectory in the inertial reference frame.

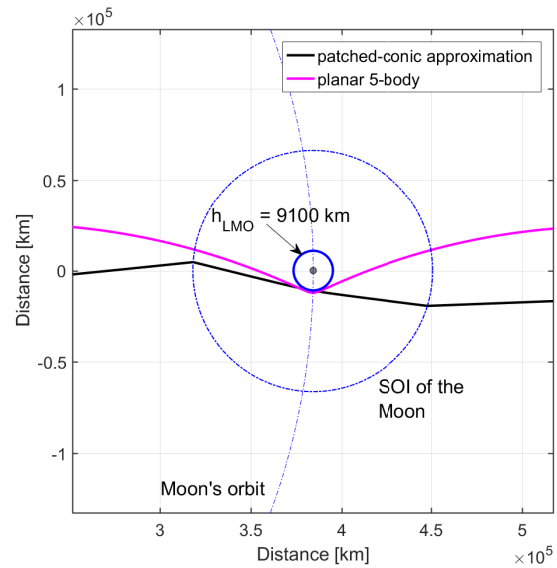


Figure 6: Zoom at the lunar swing-by in the Earth-Moon rotating reference frame. h_{LMO} is the swing-by closest approach altitude.

5. CONCLUSIONS

This work formulates two-point boundary values problems to determine interplanetary trajectories with and without lunar swing-by maneuvers considering several models: patched-conic approximations, four-body problem, and five-body problem. For the results, Earth-Mars and Earth-Venus trajectories are computed, which shows that the saving of fuel consumption due to the lunar swing-by maneuver is substantial with no greater changes in the time of flight. This saving of fuel consumption is observed both in patched-conic approximation with lunar swing-by maneuver and in the PCR5BP model.

6. ACKNOWLEDGEMENTS

This research is supported by grant 2019/14495-8, São Paulo Research Foundation (FAPESP). This research is supported by grant 2012/25308-5, São Paulo Research Foundation (FAPESP). This research is also supported by CAPES and by CNPq under contract 301875/2017-0.

7. REFERENCES

- Bate, R.R., Mueller, D.D. and White, J.E., 1971. *Fundamentals of astrodynamics*. Courier Dover Publications, New York. ISBN 0486600610.
- Broucke, R., 1988. “The celestial mechanics of gravity assist”. In *Proceedings... AIAA/AAS Astrodynamics Conference*, AIAA, Reston, pp. 69–78.
- Cichan, T., Bailey, S.A., Norris, S.D., Chambers, R.P., Jolly, S.D. and Scott, A., 2016. “Mars base camp: A martian moon human exploration architecture”. In *Proceedings... AIAA SPACE Forum*, AIAA, Reston.
- Daukantas, P., 2017. “Breakthrough starshot”. *Optics and Photonics News*, Vol. 28, No. 5, pp. 26–33.
- Gagg Filho, L.A. and da Silva Fernandes, S., 2015. “Optimal round trip lunar missions based on the patched-conic approximation”. *Computational and Applied Mathematics*, pp. 1–35. ISSN 1807-0302.
- Gagg Filho, L.A. and da Silva Fernandes, S., 2018. “Interplanetary patched-conic approximation with an intermediary swing-by maneuver with the moon”. *Computational and Applied Mathematics*, Vol. 37, No. 1, pp. 27–54. ISSN 1807-0302. doi:10.1007/s40314-017-0529-7. URL <https://doi.org/10.1007/s40314-017-0529-7>.
- Jones, D.R., 2016. “Trajectories for europa flyby sample return”. In *Proceedings... AIAA/AAS Astrodynamics Specialist Conference*, AIAA, Reston.
- Konstantinidis, K., Martinez, C.L.F., Dachwald, B., Ohndorf, A., Dykta, P., Bowitz, P., Rudolph, M., Digel, I., Kowalski, J., Voigt, K. and Forstner, R., 2015. “A lander mission to probe subglacial water on saturn’s moon enceladus for life”. *Acta Astronautica*, Vol. 106, pp. 63 – 89. ISSN 0094-5765.
- Marec, J.P., 1979. *Optimal space trajectories*. Elsevier, New York, NY. ISBN 0444601074.
- Miele, A., Huang, H.Y. and Heideman, J.C., 1969. “Sequential gradient-restoration algorithm for the minimization of constrained functions—ordinary and conjugate gradient versions”. *Journal of Optimization Theory and Applications*, Vol. 4, No. 4, pp. 213–243. ISSN 1573-2878.
- Miele, A. and Wang, T., 1999. “Optimal transfers from an earth orbit to a mars orbit”. *Acta Astronautica*, Vol. 45, No. 3, pp. 119–133. ISSN 0094-5765.
- Prussing, J.E. and Conway, B.A., 1993. *Orbital mechanics*. Oxford University Press, New York.

8. RESPONSIBILITY NOTICE

The authors are the only responsible for the printed material included in this paper.